18

Control of the photoluminescence lifetime of quantum dots by engineering their shell structure

© P.S. Samokhvalov[1,2]¶, A.V. Karaulov[3], I.R. Nabiev[2,3,4]

[1] Laboratory of Nanobioengineering, National Research Nuclear University MEPhI (Moscow Engineering Physics Institute), 115409 Moscow, Russia
[2] LIFT Center, Skolkovo, 121205 Moscow, Russia
[3] Laboratory of Immunopathology, Department of Clinical Immunology and Allergology, Sechenov University, 119992 Moscow, Russia
[4] Laboratoire de Recherche en Nanosciences (LRN-EA4682), Universite de Reims Champagne-Ardenne, 51100 Reims, France

¶ e-mail: p.samokhvalov@gmail.com

Received September 14, 2023
Revised September 20, 2023
Accepted September 28, 2023

Quantum dots (QDs) are semiconductor nanocrystals with outstanding photoluminescence (PL) characteristics: a PL quantum yield as high as 100%, a small PL emission bandwidth, and a high emission brightness. Due to these properties, QDs have a wide range of prospective applications in optoelectronics, quantum technologies, and biomedicine. The PL lifetime is one of the most important characteristics of QDs and a crucial parameter for their applicability in many specific areas of science and technology. Although this characteristic varies widely for QDs of different chemical compositions and structures, the most common type of QDs based on CdSe cores rarely has a lifetime longer than 30 ns. In this study, an effective method for increasing the QD PL lifetime is proposed. This method consists in the formation of a gradient shell on the surface of CdSe cores, which creates a potential well for excited charge carriers. This approach makes it possible to fabricate QDs with an average PL lifetime of about 100 ns, which is more than three times higher than this parameter for the best samples of such materials reported in the literature.

Keywords: semiconductor nanocrystals, quantum dots, shell, photoluminescence, fluorescence, lifetime.

DOI: 10.61011/EOS.2023.09.57349.5586-23

Introduction

Semiconductor fluorescent nanocrystals (quantum dots, QDs) are essential both for fundamental multidisciplinary research and for practical applications in various branches of science and technology. Their unique properties, which are attributable to the quantum size effect [1,2] and a small physical size, include high quantum yields (QYs) of photoluminescence (PL), narrow PL emission spectra, the possibility to excite PL in a wide spectral window, a high emission brightness, large cross sections of two-photon absorption, and photostability under intense and long-term irradiation. Most progress has been made recently in optoelectronic (e.g., displays and light-emitting diodes [3,4]) and biomedical QD applications [5–8]. The possibility of altering the PL properties of QD by fabricating hybrid plasmon–exciton systems based on them [9] or introducing QDs into various types of microcavities [10,11] also attracts researchers' interest.

The average PL lifetime, which characterizes the efficiency of radiative recombination and reflects various PL quenching processes and channels of nonradiative energy transfer [12], is one of the key parameters of QDs. Different types of QDs have PL lifetimes that differ by several orders of magnitude: for example, QDs based on CdSe cores have a characteristic PL lifetime of 20−30 ns, while this value for PbS-based QDs may reach several μs [13]. This variation of PL lifetimes may be used in experiments on time-resolved cell imaging [14] to separate reliably the effective signal from autofluorescence of tissues. At the same time, the mixing of QDs of different compositions in experiments of this kind may induce side effects related to the differences in their toxicity, photostability, efficiency of excitation, or surface properties [15]. Although QDs based on a single material are preferable for such experiments, it often proves impossible to achieve wide PL lifetime variations in this case.

The field of quantum technology has enjoyed rapid progress in recent decades. A quantum bit (qubit) is the basic unit of quantum data. Photonic qubits are used in the majority of modern quantum informatics protocols [16]. Light sources for quantum informatic applications (quantum emitters, QEs) need to have certain photon statistics. The parameters most important for an ideal QE are high purity of single-photon emission, indistinguishability of photons, high operation speed, and high brightness. Current QE development efforts are focused on cold atoms and ions, superconducting circuits, solid-state sources (e.g., emission

centers in diamonds), and QDs [17]. Although QDs are promising materials for single-photon QEs, nanocrystals based on CdSe cores, which are the most efficient in terms of their key optical properties, have relatively short PL lifetimes, which make them ill-suited for quantum computation (owing to their correspondingly short coherence times). Thus, an enhancement of the PL lifetime of QDs based on CdSe cores is likely to have a beneficial effect on the prospects of these materials in quantum technology.

Ghosh et al. [18] provide a striking illustration of the possibility to adjust the QD PL lifetime. It has been demonstrated that the PL lifetime in a CdSe/CdS system increases sharply due to carrier delocalization in the shell when a threshold shell volume is reached. An approximately twofold PL lifetime enhancement and the related suppression of blinking are achieved only when the shell volume reaches a level of $\sim 750\,\text{nm}^3$, which corresponds to a QD diameter in excess of 11 nm.

In the present study, an alternative approach to control over the PL lifetime of QDs based on CdSe cores, which involves the formation of a gradient shell that produces a potential well for excited charge carriers, is proposed. This shell structure has an advantage over a thick shell with a flat potential in allowing a more efficient exciton delocalization, which provides an opportunity to raise the QD PL lifetime by a factor of more than 3 while keeping the nanocrystal volume below $750\,\text{nm}^3$.

Experimental

Materials

The following materials were used to synthesize QDs: cadmium oxide (99.5%), zinc oxide (99.99%), 1-octadecene (ODE, 90%), oleylamine (OA, 70%), selenium (99.5%), thiourea ($\geq 99.0\%$), trioctylphosphine (TOP, 97%), trioctylphosphine oxide (TOPO, 99%), 2-ethylhexanoic acid (2-EHA, 99%), trioctylamine (TOA, 98%), triglyme (99%), and anhydrous solvents (chloroform, n-hexane, and methyl acetate). All these reagents were purchased from Sigma-Aldrich. n-Hexadecylphosphonic acid (HDPA, 97%) was purchased from PlasmaChem GmbH. All reagents were used without further purification.

Synthesis

The synthesis of QDs with the CdSe(core)/ZnS/CdS/ZnS(multilayer shell) structure (CdSe/MS) was discussed in detail in [19]. The production of these QDs and QDs with a gradient shell started with the injection synthesis of CdSe cores in an ODE medium, with trioctylphosphine selenide and cadmium n-hexadecylphosphonate used as precursors. The precursor and reaction medium residues were removed from the surface of the synthesized cores by gel permeation chromatography [20], and the cores were then treated with OA and introduced into the medium for shell deposition (a mixture of ODE and OA at a volume ratio of 1 : 1). Shells were grown by the layer-by-layer method at a temperature of 165–180°C, with a solution of thiourea in triglyme and zinc and cadmium 2-ethylhexanoates used as precursors. Precisely measured amounts of the precursors for growth of each shell layer were added automatically with syringe pumps. The reaction time for each monolayer fell within the range of 10–60 min. When the synthesis was complete, QDs were isolated from the reaction medium by precipitating the colloidal solution with methyl acetate and subsequent centrifugation. The QDs were then rinsed additionally with various combinations of solvents and dried in a mixture with TOPO, which served as an inert matrix. Prior to measurements, excess TOPO was removed from the samples, and solutions of QDs in different solvents were prepared.

Instrumental methods

Quartz cuvettes with an optical path length of 10 mm were used to record the absorption and PL spectra of QD solutions with a Cary 60 (Agilent, United States) and a Cary Eclipse (Agilent, United States) spectrometers, respectively. Chloroform and n-hexane were used as solvents for these measurements. The QY of photoluminescence was measured relative to the Rhodamine 6G dye (with a QY of 0.95) in accordance with the procedure detailed in [21]. The optical densities of the solutions at the excitation wavelength were kept below 0.1 so as to avoid internal filtering.

Transmission electron microscopy (TEM) studies were performed using a JEOL JEM-2100F (JEOL, Japan) microscope at an accelerating voltage of 200 kV. The samples for them were prepared by depositing $5\,\mu$l of a solution of QDs in toluene onto copper meshes for microscopy (200 mesh) coated with amorphous carbon and Formvar polymer layers.

Time-resolved studies of QD PL were carried out using a setup consisting of a pulsed picosecond laser with a radiation wavelength of 405 nm (PicoQuant, Germany), a Taiko laser driver (PicoQuant, Germany), an avalanche photodiode (MPD), a PicoHarp 300 multichannel single-photon counting system (PicoQuant, Germany), an M266 monochromator (Solar Laser Systems, Belarus), and an HR2000+ modular spectrometer (Ocean Optics, United States). A laser with a pulse repetition rate of 10 kHz and a pulse power of $18\,\mu$W was used to excite the solutions of samples in n-hexane. PL decay curves for time-resolved PL spectra were recorded with a fixed exposure time (15 min), a resolution of 512 ps, and a transmission wavelength varying within the 500–650 nm interval with a step of 10 nm. The obtained data set was subjected to mathematical processing to find the base line of each curve. Kinetic data were then converted into PL spectra by interpolating the PL signal intensity values from time-resolved curves at a given time point from the moment of the maximum signal intensity at 560 nm, which was fixed for all kinetic curves and was assumed to be the origin of time, to a time of 1000 ns in 25 ns steps.

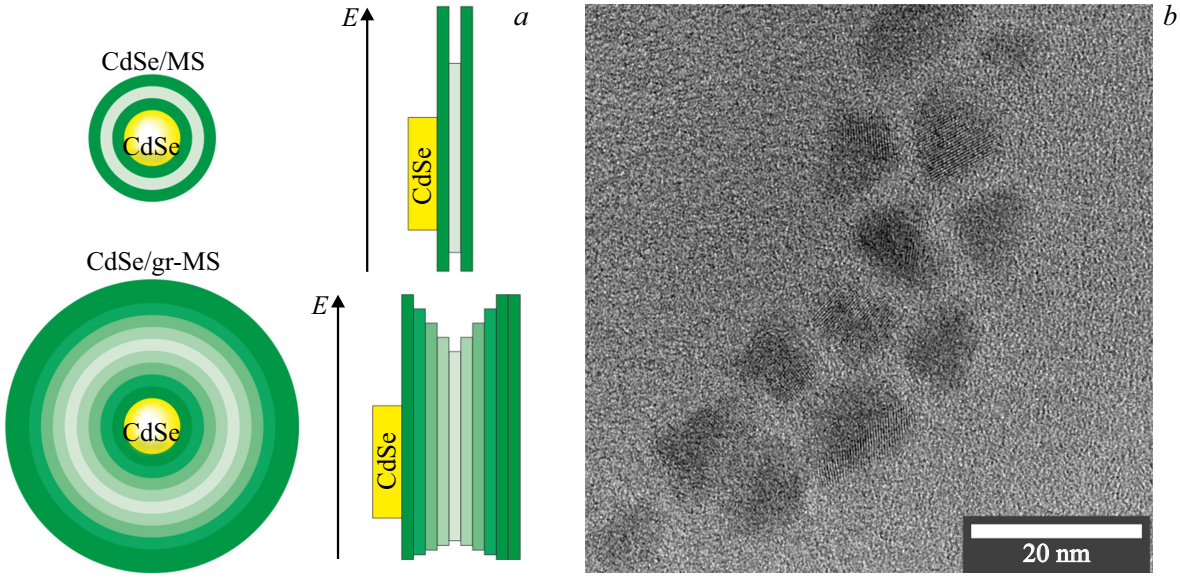

Figure 1. Schematic diagram of the QD structure and the results of TEM studies of CdSe/gradient MS (gr-MS) QDs. (*a*) Schematic structure and energy diagrams of QDs with a CdSe core and a ZnS/CdS/ZnS shell with a thickness of 3 monolayers (CdSe/MS) and QDs with a gradient shell with an overall thickness of 10 monolayers (CdSe/gr-MS); (*b*) TEM image of a CdSe/gr-MS QD sample.

Results and discussion

As a noted above the average PL lifetime of CdSe-based QDs normally does not exceed 20–30 ns. Specifically, the PL lifetime in studies reporting successful synthesis of QDs with a PL QY close to 100% (see, e.g., [22]) is 32 ns. This value was raised to 37 ns when a thick gradient $Cd_xZn_{1-x}S$ shell was deposited onto CdSe cores [23]. A CdS shell thicker than 10 monolayers deposited onto CdSe cores allows strong delocalization of excited charge carriers between the core and the shell, thus enhancing the PL lifetime [18]. It was demonstrated in the cited paper that the average PL lifetime increased to about 65 ns when a threshold shell volume of $\sim 750\,nm^3$ was exceeded; the maximum value of 152 ns was achieved in experiments with QDs with a core diameter of 3.0 nm and 20 CdS shell layers. Thus, such a significant lifetime enhancement required the use of QDs with an overall diameter above 17 nm. It is also important that the transition to long PL lifetimes is accompanied by a significant suppression of blinking [18].

Our approach to extending the QD PL lifetime differs from the ones proposed in earlier studies and consists in creating a conformal CdSe shell that has a gradient structure with the chemical composition varying gradually as ZnS→CdS→ZnS (Fig. 1, *a*), around the CdSe core. We assume that this should help produce a potential well for excited charge carriers, thus inhibiting their radiative recombination. These new QDs differ from the CdSe(core)/ZnS/CdS/ZnS(multilayer shell) QDs fabricated in our earlier studies [19,24,25], where the thickness of each shell layer was made exactly equal to one monolayer of the corresponding material, in having slightly lower barrier potentials (due to alloying), but feature a significantly expanded volume available for delocalization. The energy structure of the shell (Fig. 1, *a*), which has a relatively high potential barrier between the core and the shell center, should also slow down the return of carriers to the core and act in concert with an enhanced shell thickness toward extending the time of delocalization of excited carriers.

Cadmium selenide cores 2.3 nm in diameter were synthesized to verify these assumptions. The obtained sample was divided into two parts, and shells of the corresponding structure were deposited onto both of them. Below the QD sample with a CdSe core and a ZnS/CdS/ZnS shell with a thickness of 3 monolayers (ML) is denoted as CdSe/MS, and the sample with a gradient shell with an overall thickness of 10 ML is denoted as CdSe/gr-MS. Figure 1, *b* presents the TEM image of the prepared CdSe/gr-MS QDs. The obtained nanocrystals had an irregular tetrahedron-like shape; the mean QD size was 10.7 ± 1.7 nm.

Figure 2 shows the optical absorption and PL spectra for the prepared materials. It can be seen that the PL spectra of two types of QDs have very close characteristics: for example, the PL maximum for the CdSe/MS sample is located at 560 nm, with a FWHM of 47.1 nm, while the respective parameters for CdSe/gr-MS QDs are 564 and 49.9 nm. In contrast, the absorption spectra of the samples differ clearly: although the positions of the first exciton absorption maximum match almost perfectly (these maxima are located approximately at 535 nm), the absorbance of the CdSe/gr-MS sample in the blue and UV spectral regions is much higher, since its shell is thicker and, consequently, has a greater absorption cross section. These samples also have different PL QY values: the QY for the CdSe/MS sample with a thinner shell is 93%, while the CdSe/gr-MS QDs have a QY as low as 30%. This difference

Results of approximation of PL decay curves and calculation of average PL lifetimes for CdSe/MS and CdSe/gr-MS QDs

QD type	A_1	τ_1, ns	A_2	τ_2, ns	A_3	τ_3, ns	τ_{av}, ns
CdSe/MS	0.925 ± 0.009	22.3 ± 0.2	0.06 ± 0.01	67 ± 6	–	–	29 ± 9
CdSe/gr-MS	0.639 ± 0.006	37.2 ± 0.6	0.152 ± 0.007	7.5 ± 0.5	0.184 ± 0.005	151 ± 3	96 ± 17

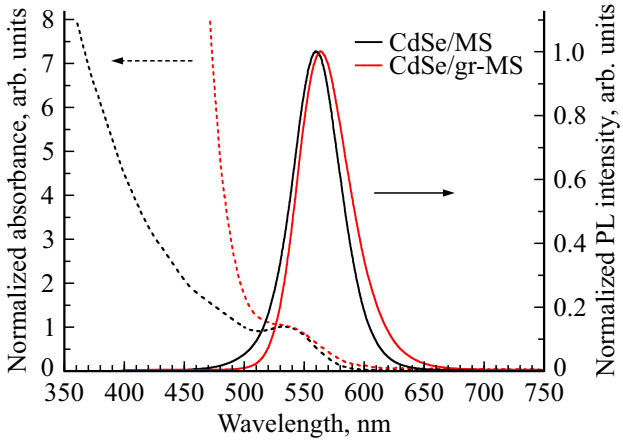

Figure 2. Optical absorption spectra (dashed curves) and PL spectra (solid curves) of CdSe/MS QDs (black curves) and CdSe/gr-MS QDs (red curves).

is attributable to the fact that the time interval of synthesis of QDs with a thicker shell is three times longer than the one for CdSe/MS QDs. It is important that spontaneous charge transfer between the inorganic QD part and the ligand shell or the ambient environment may occur in the process of shell growth at a fairly high temperature (165–180°C) [26], sending a nanocrystal into a nonradiating „dark" state. The probability of transition of a significant fraction of QDs to this state rises with increasing reaction time, while a gradual increase in the shell thickness reduces the probability of QD neutralization as a result of reverse charge transfer. However, it should be noted that this problem is not an insurmountable one and can be resolved by optimizing the synthesis conditions.

The comparison of PL decay kinetics of two types of QDs (Fig. 3, *a*) revealed that the proposed approach provides a significant enhancement of the PL lifetime of QDs based on cadmium selenide. The QD PL lifetime was calculated by approximating the decay curves with bi- and tri-exponential functions of the form

$$I(t) = \sum_i^n A_i e^{-t/\tau_i}, \qquad (1)$$

where n is the number of exponential functions in the approximation, A_i is the pre-exponential factor, and τ_i is the characteristic decay time of each exponential function. The characteristic PL lifetime was then calculated as an intensity-weighted average (τ_{av}) in the following way [27]:

$$\tau_{av} = \sum_i^n A_i \tau_i^2 \Big/ \sum_i^n A_i \tau_i. \qquad (2)$$

The results of approximation and calculated average PL lifetimes for two types of QDs are listed in the table. It should be noted that the PL decay curve for CdSe/MS QDs can also be approximated fairly well by a mono-exponential function within the 0–100 ns interval. The average lifetime determined in this way is 24.1 ns. This is indicative of fine quality of the prepared material and suggests that the fast decay component, which is commonly associated with nonradiative excitation relaxation channels, is suppressed almost completely.

Comparison of the average PL lifetimes for CdSe/MS and CdSe/gr-MS QDs shows that the proposed approach indeed provides an opportunity to raise the lifetime of the excited state by a factor of 3 via temporary delocalization of excited carriers in a potential well created by the gradient shell. It should be noted that three characteristic lifetimes of the excited state obtained by approximating the PL decay curve for CdSe/gr-MS QDs are 37.2, 7.5, and 97 ns. The first and the third values correspond roughly to two lifetimes from the approximation of the curve for CdSe/MS QDs and may be related to the direct radiative recombination of excitons in CdSe cores (approximately 30 ns) and the recombination of charge carriers delocalized in shells (> 60 ns). The lower degree of delocalization in CdSe/MS QDs translates into a shorter decay time of delocalized states. The second (fast) PL decay component of CdSe/gr-MS QDs may be related to the rapid recombination in QDs with an excess negative charge in the so-called „grey" state [26,28].

Figure 3, *b* presents the time-resolved PL spectra of the new type of QDs. These spectra were plotted by processing PL decay curves recorded at different transmission wavelengths of the monochromator. It can be seen that the spectral position of the emission maximum remains almost unchanged: only a slight red shift from 550 to 562 nm is seen within the 0–1000 ns interval. This observation confirms the assumption that radiative recombination occurs only in the core of CdSe/gr-MS QDs, where the energy of carriers is the lowest.

Thus, an efficient method for controlling the average QD PL lifetime has been proposed. This opens up new opportunities for application of these materials in quantum computing and biomedicine. It has been demonstrated using the example of a new type of QDs with a gradient

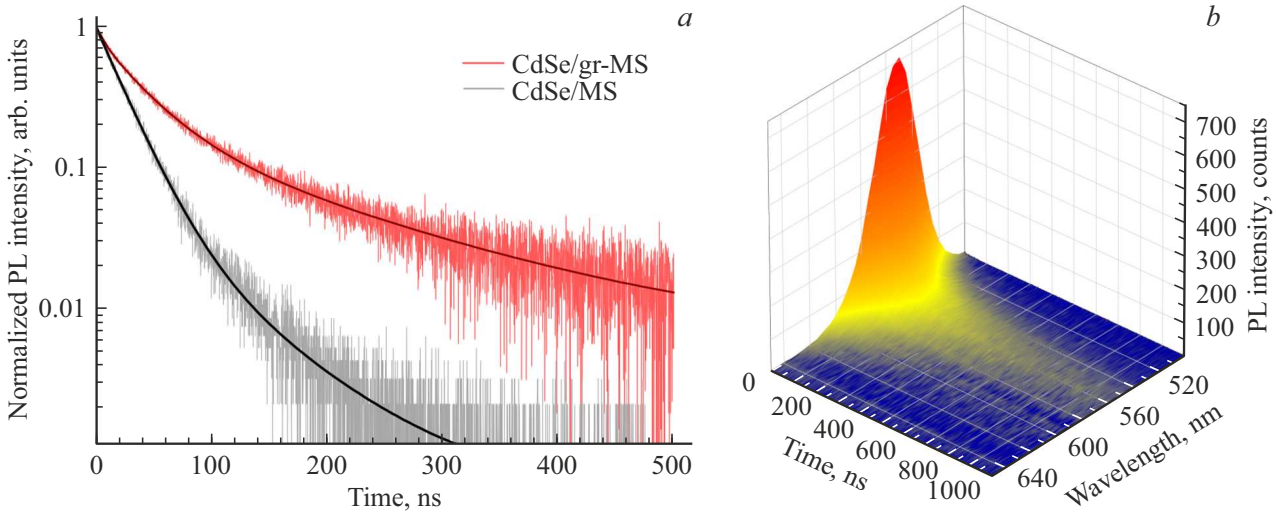

Figure 3. Time-resolved PL characteristics of CdSe/MS and CdSe/gr-MS QDs. (*a*) QD PL decay curves and their approximations with polyexponential functions (thick curves are the results of approximation); (*b*) time-resolved PL spectra of CdSe/gr-MS QDs within the 0–1000 ns interval.

shell, which creates an additional potential well with smooth edges, that the recombination time of excited charge carriers may be extended by a factor of more than 3. The fabricated QDs are relatively small-sized, and, to the best of our knowledge, the mentioned PL lifetime enhancement is greater than the anyone reported to date.

Conclusion

A novel approach to enhancing the QD PL lifetime by fabricating QDs with a gradient shell, which creates a potential well for charge carriers and extends the time of their delocalization, has been proposed and implemented. This extended delocalization gives rise to a „long" exponential component in PL decay curves but does not alter the PL emission spectrum. It should be noted that a more than threefold enhancement of the average PL lifetime was achieved in QDs with an overall shell thickness of 10 monolayers, which is significantly thinner than the threshold shell thickness required for the weaker effect of PL kinetics elongation. This confirms the efficiency of the proposed approach and suggests that QDs of the new type can be used in time-resolved bioimaging and quantum computing. The application of this approach to QDs with other cores having intrinsically longer PL lifetimes (e.g., $CuInS_2$ or PbS) should make it possible to achieve an even stronger deceleration of PL kinetics, to several tens or hundreds of μs, making these objects viable competitors to other current technologies for cubit production.

Funding

This study was supported by the Ministry of Science and Higher Education of the Russian Federation, agreement No. 075-15-2021-937 (NanoToBio project).

Conflict of interest

The authors declare that they have no conflict of interest.

References

[1] L.E. Brus. J. Chem. Phys., **80**, 4403–4409 (1984). DOI: 10.1063/1.447218
[2] P. Samokhvalov, M. Artemyev, I. Nabiev. Chem.–A Eur., **19**, 1534–1546 (2013). DOI: 10.1002/chem.201202860
[3] A.P. Litvin, I.V. Martynenko, F. Purcell-Milton, A.V. Baranov, A.V. Fedorov, Y.K. Gun'ko. J. Mater. Chem. A, **5**, 13252–13275 (2017). DOI: 10.1039/C7TA02076G
[4] Z. Chen, H. Li, C. Yuan, P. Gao, Q. Su, S. Chen. Small Methods, (2023). DOI: 10.1002/smtd.202300359
[5] A. Sukhanova, K. Even-Desrumeaux, A. Kisserli, T. Tabary, B. Reveil, J.-M. Millot, P. Chames, D. Baty, M. Artemyev, V. Oleinikov, M. Pluot, J.H.M. Cohen, I. Nabiev. Nanomedicine: NBM, **8**, 516–525 (2012). DOI: 10.1016/j.nano.2011.07.007
[6] R. Bilan, F. Fleury, I. Nabiev, A. Sukhanova. Bioconjug. Chem., **26** (4), 609–624 (2015). DOI: 10.1021/acs.bioconjchem.5b00069
[7] P. Sokolov, P. Samokhvalov, A. Sukhanova, I. Nabiev. Nanomaterials, **13** (11), 1748 (2023). DOI: 10.3390/nano13111748
[8] W.R. Algar, M. Massey, K. Rees, R. Higgins, K.D. Krause, G.H. Darwish, W.J. Peveler, Z. Xiao, H.-Y. Tsai, R. Gupta, K. Lix, M.V. Tran, H. Kim. Chem. Rev., **121**, 9243–9358 (2021). DOI: 10.1021/acs.chemrev.0c01176

[9] V. Krivenkov, P. Samokhvalov, I. Nabiev, Y.P. Rakovich. J. Phys. Chem. Lett., **11**, 8018–8025 (2020). DOI: 10.1021/acs.jpclett.0c02296
[10] D. Dovzhenko, V. Krivenkov, I. Kriukova, P. Samokhvalov, A. Karaulov, I. Nabiev. Opt. Lett., **45**, 5364 (2020). DOI: 10.1364/OL.400300
[11] D. Dovzhenko, M. Lednev, K. Mochalov, I. Vaskan, P. Samokhvalov, Y. Rakovich, I. Nabiev. Appl. Phys. Lett., **119**, 011102 (2021). DOI: 10.1063/5.0047146
[12] C. Galland, Y. Ghosh, A. Steinbrück, J.A. Hollingsworth, H. Htoon, V.I. Klimov. Nat. Commun., **3**, 908 (2012). DOI: 10.1038/ncomms1916
[13] D. Borrero Landazabal, A.A. Meza Olivo, K. Garay Palmett, R. Salas Montiel. J. Phys. Conf. Ser., **1159**, 012004 (2019). DOI: 10.1088/1742-6596/1159/1/012004
[14] B. Zhang, C. Yang, Y. Gao, Y. Wang, C. Bu, S. Hu, L. Liu, H.V. Demir, J. Qu, K.-T. Yong. Nanotheranostics, **1**, 131–140 (2017). DOI: 10.7150/ntno.18989
[15] A. Sukhanova, S. Bozrova, E. Gerasimovich, M. Baryshnikova, Z. Sokolova, P. Samokhvalov, C. Guhrenz, N. Gaponik, A. Karaulov, I. Nabiev. Nanomaterials, **12**, 2734 (2022). DOI: 10.3390/nano12162734
[16] S. Slussarenko, G.J. Pryde. Appl. Phys. Rev., **6** (2019). DOI: 10.1063/1.5115814
[17] C.R. Kagan, L.C. Bassett, C.B. Murray, S.M. Thompson. Chem. Rev., **121**, 3186–3233 (2021). DOI: 10.1021/acs.chemrev.0c00831
[18] Y. Ghosh, B.D. Mangum, J.L. Casson, D.J. Williams, H. Htoon, J.A. Hollingsworth. J. Am. Chem. Soc., **134** (23), 9634–9643 (2012). DOI: 10.1021/ja212032q
[19] P. Samokhvalov, P. Linkov, J. Michel, M. Molinari, I. Nabiev. In: *Colloidal Nanoparticles for Biomedical Applications IX,* ed. by W.J. Parak, M. Osinski, K.I. Yamamoto. Proc. SPIE, **8955**, 89550S (2014). DOI: 10.1117/12.2040196
[20] P.A. Linkov, K.V. Vokhmintcev, P.S. Samokhvalov, I.R. Nabiev. Opt. Spectrosc., **122** (1), 8–11 (2017). DOI: 10.7868/S0030403417010160
[21] C. Würth, M. Grabolle, J. Pauli, M. Spieles, U. Resch-Genger. Nat. Protoc., **8** (8), 1535–1550 (2013). DOI: 10.1038/nprot.2013.087
[22] O. Chen, J. Zhao, V.P. Chauhan, J. Cui, C. Wong, D.K. Harris, H. Wei, H.-S. Han, D. Fukumura, R.K. Jain, K. Rakesh, B.G. Moungi. Nat. Mater., **12** (5), 445–451 (2013). DOI: 10.1038/nmat3539
[23] K. Boldt, N. Kirkwood, G.A. Beane, P. Mulvaney. Chem. Mater., **25** (23), 4731–4738 (2013). DOI: 10.1021/cm402645r
[24] P. Linkov, V. Krivenkov, I. Nabiev, P. Samokhvalov. Mater. Today Proc., **3** (2), 104–108 (2016). DOI: 10.1016/j.matpr.2016.01.033
[25] V. Krivenkov, S. Goncharov, P. Samokhvalov, A. Sánchez-Iglesias, M. Grzelczak, I. Nabiev, Y. Rakovich. J. Phys. Chem. Lett., **10**, 481–486 (2019). DOI: 10.1021/acs.jpclett.8b03549
[26] V. Krivenkov, P. Samokhvalov, M. Zvaigzne, I. Martynov, A. Chistyakov, I. Nabiev. J. Phys. Chem. C, **122**, 15761–15771 (2018). DOI: 10.1021/acs.jpcc.8b04544
[27] Y. Li, S. Natakorn, Y. Chen, M. Safar, M. Cunningham, J. Tian, D.D.-U. Li. Front. Phys., **8** (2020). DOI: 10.3389/fphy.2020.576862
[28] F. Gao, P. Bajwa, A. Nguyen, C.D. Heyes. ACS Nano, **11** (3), 2905–2916 (2017). DOI: 10.1021/acsnano.6b08040

Translated by D.Safin